Effect of Styrene-Maleic Anhydride as a Reactive Compatibilizer on the Mechanical Properties and Flammability of Intumescent Flame Retardant Polystyrene

Yajun Chen,[1,2] Zhenghong Guo,[2] Zhengping Fang[1,2]

[1]*Key Laboratory of Macromolecular Synthesis and Functionalization, Institute of Polymer Composites, Zhejiang University, Ministry of Education, Hangzhou 310027, People's Republic of China*
[2]*Laboratory of Polymer Materials and Engineering, Ningbo Institute of Technology, Zhejiang University, Ningbo 315100, People's Republic of China*

Received 28 September 2009; accepted 14 March 2010
DOI 10.1002/app.32452
Published online 14 May 2010 in Wiley InterScience (www.interscience.wiley.com).

ABSTRACT: Polystyrene (PS) was flame retarded with a polymeric intumescent flame retardant, poly(diaminodiphenyl methane spirocyclic pentaerythritol bisphosphonate) (PDSPB), and *in situ* compatibilized with styrene-maleic anhydride (SMA) copolymer. Compatibilization reaction was verified by IR spectroscopy and gel content measurement. Electron microscopy images showed that compatibilization could considerably reduce the size of the flame retardant domains and improve the interfacial adhesion between PS and PDSPB. With the same PDSPB loading (20 wt %), addition of 5, 10, and 20 wt % SMA increased the impact strength of the flame retarded PS by about 29, 103, and 201%, respectively. Compared with PS/PDSPB sample, addition of 5 wt % of SMA improved the limiting oxygen index from 23.8 to 24.2 and reduced the peak heat release rate (PHRR) of the blend by 18.3%. However, further increment of SMA content deteriorated the flame retardancy of the blend. It was found that the $-NH_2$ groups changed into more stable imide groups at high temperature, causing the absence of gas source. Therefore, the intumescent char could not be formed during combustion process, which was the main reason for the deteriorate effect of flame retardancy at high SMA loading. © 2010 Wiley Periodicals, Inc. J Appl Polym Sci 118: 152–158, 2010

Key words: polystyrene; styrene-maleic anhydride copolymer; compatibility; mechanical property; flammability

INTRODUCTION

Most of the current flame retardant plastics are mixtures composed of polymers, flame retardants, additives, or fillers. As these polymer materials are mixtures with a multiphase morphological structure, the miscibility and the adhesion on the interface act as key characteristics for the physical properties and performance of these materials.[1–4]

Halogen-free flame retardant has attracted much attention by both scientists and engineers in recent years due to the ecological problems caused by traditional halogen flame retardants. Intumescent flame retardants (IFRs) are preferably used in thermoplastics due to their advantages of little smoke release and low toxicity.[5,6]

A novel phosphorous nitrogen-containing IFR, that is, poly(diaminodiphenyl methane spirocyclic pentaerythritol bisphosphonate) (PDSPB) was synthesized in our laboratory and proved to be an efficient IFR.[7–9] Although the flame retardancy property of PDSPB in polystyrene (PS) is outstanding in our previous work,[10] it also causes some problems, such as phase separation and weak interfacial adhesion because of the rather different polarities between PS and PDSPB. As a result, the mechanical properties and flammability of IFR-PS were not satisfied.

Reactive compatibilization[11–15] has been proved to be an effective method to improve the interfacial adhesion and morphology control in a variety of incompatible blends. However, reactive compatibilization may affect the flammability in IFR system because the functional groups of IFR could react with compatibilizer.

In this study, styrene-maleic anhydride (SMA) copolymers which are frequently used in reactively compatibilized blend systems[16–18] was used as a compatibilizer to modify the interfacial adhesion between PS matrix and PDSPB particles. The effect of SMA on the properties of IFR-PS was characterized. And the relationship between reactive compatibilization and flammability was discussed.

EXPERIMENTAL

Materials

The PS resin used is a general purpose grade transparent resin, manufactured by Yanshan Petrochemical

Correspondence to: Z. Fang (zpfang@zju.edu.cn).
Contract grant sponsor: National Natural Science Foundation of China; contract grant number: 50873092.

TABLE I
Formulations for Flame Retarded PS Systems

Sample code	Composition (g)		
	PS	PDSPB	SMA
PS1	100	0	0
PS2	80	20	0
PS3	75	20	5
PS4	70	20	10
PS5	60	20	20
PS6	87.5	0	12.5

Company (Beijing, China) under the trade name 666D, with molecular weight of 200,000 g/mol and polydispersity index of 2.3, as measured by GPC.

The SMA used is a random copolymer of styrene and maleic anhydride, produced by ARCO with the trade name Dylark 332. Its molecular weight and polydispersity index are reported by the manufacturer to be 180,000 g/mol and 2.0, respectively. Elemental analysis shows that Dylark 332 contained 13.9 wt % MA.

PDSPB was synthesized by condensation polymerization according to procedures published previously[7] and its structure was shown below ($n = 4$–5):

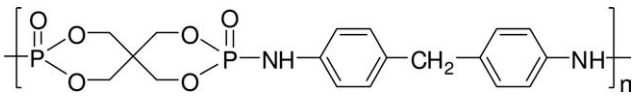

Preparation of blends

The PS/PDSPB and PS/PDSPB/SMA blends were prepared via melt compounding at 180°C in Thermo Haake Rheomix with a rotor speed of 60 rpm, and the mixing time was 8 min for each sample. The mixed samples were transferred to a mold and heated at 180°C for 3 min, then pressed at 20 MPa, and successively cooled to room temperature while maintaining the pressure to obtain the blend sheets for further measurements. The formulations prepared are shown in Table I.

Characterization

Infrared spectroscopy (IR) was applied with a Vector-22 FTIR spectrometer using KBr pellets.

The gel content measurement was performed using a Soxhlet extractor by refluxing PS, PS/SMA, PS/PDSPB, and PS/PDSPB/SMA samples, which has been shredded and wrapped in filter, in boiling xylene for 48 h.

Scanning electron microscopy (SEM) images were recorded on a SIRION-100 (FEI, Hillsboro, OR) with SEM at an accelerating voltage of 10 kV. To study the morphological behavior, the fractured surfaces of the sample were first sputter coated with a conductive layer, and then its morphologic structures were observed. The char residues after cone calorimetric measurements were first glued to the sample stage with liquid conductive adhesive and then its morphologic structures were observed.

The unnotched impact strength of the sample was tested according to GB/T2571–1995 using Charpy impact tester (XCJ-L). Five pieces were tested and averaged for each sample.

Flammability of the samples was characterized by a cone calorimeter performed with an FTT, UK device according to ISO 5660 at an incident flux of 35 kW/m^2 using a cone shaped heater. The cone data reported here were the averages of three replicated experiments.

Thermogravimetric analysis (TGA) was done in a TA SDTQ600 thermal analyzer at a scanning rate of 10°C /min under air from 30 to 600°C.

Limiting oxygen index (LOI) was also used to measure the fire retardancy. This method followed the ASTM D2863-2008 procedure, using specimens of 130 × 6.5 × 1.6 mm.

RESULTS AND DISCUSSION

Compatibilization mechanism

The active terminal $-NH_2$ groups of flame retardant PDSPB can react with the maleic anhydride groups (MAH) in SMA to generate graft copolymers, which can compatibilize the PS/PDSPB system during blend processing. The possible compatibilization reaction is shown in Scheme 1. To verify this reaction, IR and gel content measurements were performed.

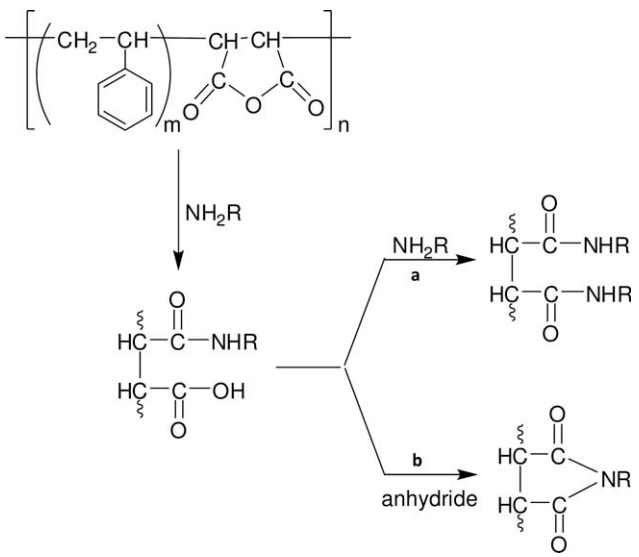

Scheme 1 The reaction between SMA and PDSPB, where R represent the main chain of PDSPB.

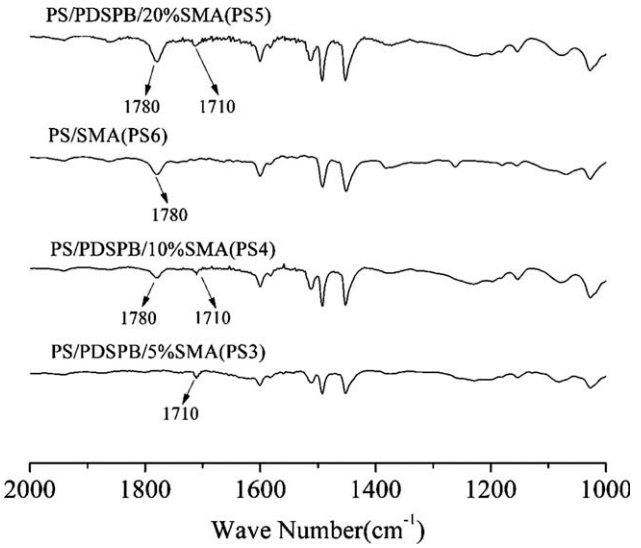

Figure 1 FTIR spectra of PS/20%PDSPB/5%SMA, PS/20%PDSPB/10%SMA, PS/20%PDSPB/20%SMA, and PS/SMA after melt blending.

The IR spectra of PS3, PS4, PS5, and PS6 after melt blending are shown in Figure 1. For the IR spectrum of the PS/SMA sample (PS6), the absorption peaks at 1780 cm^{-1} are attributed to symmetric stretching vibrations of carbonyl groups in MAH of SMA molecules. For PS/PDSPB/SMA samples (PS3, PS4, and PS5), a new absorbing band at 1710 cm^{-1} ascribes to imide group,[19,20] which indicates that a ring opening reaction has taken place. Moreover, the IR spectroscopy shows that there is no peak at 1780 cm^{-1} when the content of SMA is 5 wt % (PS3), implying that SMA has reacted completely [Scheme 1(a)]. However, both curves of the PS/PDSPB systems with 10 and 20 wt % SMA have peaks at 1780 cm^{-1}, indicating the overplus of SMA [Scheme 1(b)].

The gel content measurement can be used to prove whether the reaction has occurred because the graft copolymers generated in the compatibilization reaction are likely crosslink products and do not dissolve in boiling xylene. The gel content (g) was calculated according to the following formula:

$$g = W_1/W_0 \times 100\%$$

where W_1 is the weight of the sample after extraction and W_0 is the weight of the sample before extraction. The gel contents values of PS2, PS3, PS4, and PS5 are shown in Table II taking into account that no gels appear in PS1 and PS6 due to the complete dissolution of PS and SMA. For PS/PDSPB (PS2) sample, about 14.4% residues indicate that PDSPB can't dissolve in boiling xylene completely. For PS/PDSPB/SMA systems, the gel content increases with increasing SMA loading, 19.6, 26.6, and 33.1 wt %, respectively. Apparently, the gel content of the PS/PDSPB/SMA samples is composed of the remaining flame retardant PDSPB and the insoluble graft copolymers because it is difficult to deduct the part of remaining PDSPB. Despite this, the gel content provides powerful evidence for the compatibilization reaction.

Morphology

Morphological observations were made by using a SEM. The fracture surface after impact measurement of PS/PDSPB and PS/PDSPB/SMA blends are presented in Figure 2. These photographs show that the fractured surfaces of the PS2 and PS3 exhibit typical brittle feature [Figs. 2(a) and 1(b)], but with the increase of the SMA content (PS4 and PS5), the fractured surfaces show typical tough feature [Figs. 2(c) and 1(d)], which have higher efficiency to absorb the impact energy.

From the SEM micrographs we can see that PS is the continuous matrix in which the PDSPB particles are dispersed, which indicates that some of the PDSPB particles agglomerate together. The microparticles with a diameter of 8 μm to 10 μm seen in Figure 2(a) are PDSPB. It is clear that the adhesion between the matrix and the IFR is very poor, resulting in a distinct interface between PS matrix and PDSPB particles. The IFR surface does not have good contact with the matrix, and has voids on the fracture surface because of the breaking off of PDSPB particles. As a result, most of the PDSPB particles are almost completely separated from the matrix after impact, shown in Figure 2(a). These are the so-called defects or crack initiating points of the materials.[21] Consequently, a much lower impact strength should be obtained, which will be discussed in the next section.

Addition of SMA changes this situation, as seen in Figure 2(b–d). The PDSPB particles are embedded in PS matrix. Almost no isolated PDSPB particle appears on the fractured surfaces. The voids on the interface disappeared when SMA content exceeded 5 wt %. The diameter of PDSPB particles decrease to about 5, 2, and 1 μm, respectively, when the content of SMA increases to 5, 10, and 20 wt %. Compared with PS/PDSPB blend, addition of SMA as compatibilizer is able to induce a good dispersion and prevent the agglomeration of PDSPB, decrease the size of dispersed phase, and substantially improve the

TABLE II
Gel Contents of PS/20%PDSPB (PS2), PS/20%PDSPB/5%SMA (PS3), PS/20%PDSPB/10%SMA (PS4), and PS/20%PDSPB/20%SMA (PS5)

Sample	PS2	PS3	PS4	PS5
Gel content (%)	14.4	19.6	26.6	33.1

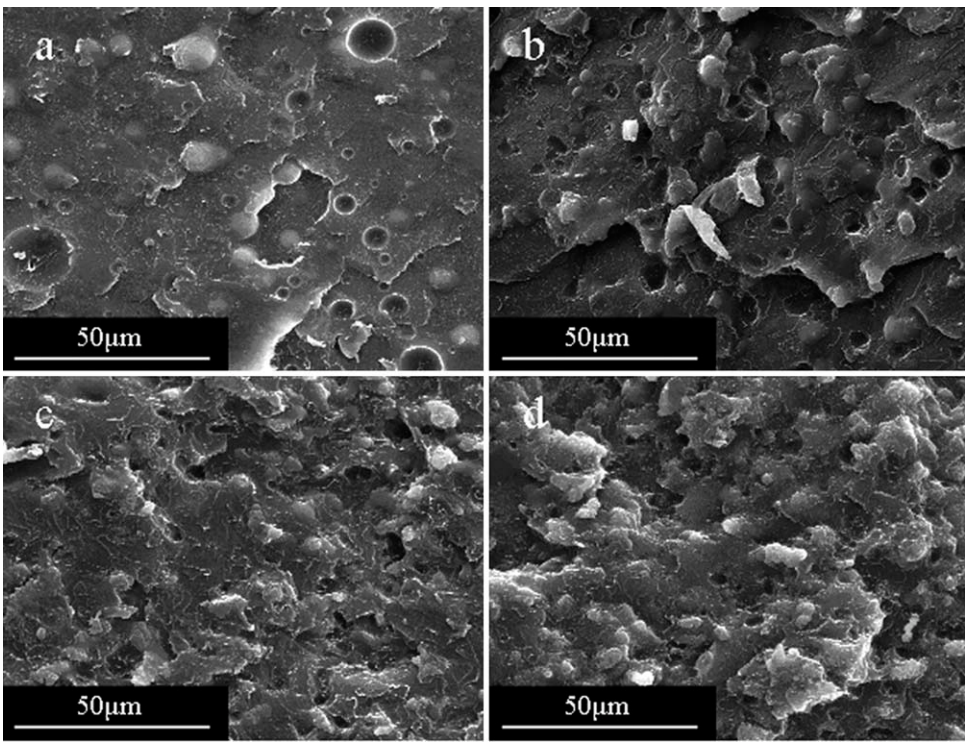

Figure 2 Morphologies of fracture surfaces for PS/20%PDSPB (a), PS/20%PDSPB/5%SMA (b), PS/20%PDSPB/10%SMA (c), and PS/20%PDSPB/20%SMA (d).

interfacial adhesion between PDSPB particles and PS matrix. The interphase becomes illegible with the increase of SMA content.

Mechanical properties

Figure 3 depicts the average impact strength of these blends with various SMA contents. The impact strength of PS6 (3.15 KJ/m^2) is higher than PS1 (2.48 KJ/m^2), which implies that SMA is able to provide better impact resistance. With the same IFR loading (20 wt %), addition of SMA into PS/PDSPB blends led to improvement in impact strength. Moreover, with 5, 10, and 20 wt % SMA loadings, the impact strength increased about 29, 103, and 201%, respectively compared with the PS/PDSPB blend. This indicates that the interface between the matrix and PDSPB particle is no longer the defect or crack initiating point of the material. The reason is that the interphase formed by SMA between PS and PDSPB acts as an energy absorbing phase, and is able to entangle with the PS matrix. The interphase becomes thicker with the increase of SMA contents (from 5 to 20 wt %). When the addition of SMA is up to 20 wt %, there must be many chains of SMA that do not react to the surface of PDSPB, increase the degree of freedom of the intramolecular motion of SMA.[22,23] Therefore, the blend with 20 wt % SMA provides the highest impact resistance of all. Therefore, it can be concluded that increasing the SMA weight fraction in blends improves the impact strength significantly.

Flammability properties

Cone calorimetry is widely used to evaluate fire performance. It is one of the most effective bench-scale methods for studying the flammability properties of materials. Various parameters are obtained from

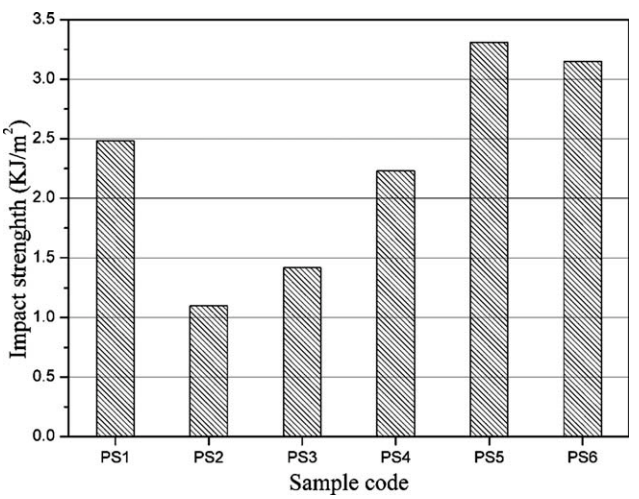

Figure 3 Impact strength of pure PS (PS1), PS/20%PDSPB (PS2), PS/20%PDSPB/5%SMA (PS3), PS/20%PDSPB/10%SMA (PS4), PS/20%PDSPB/20%SMA (PS5), and PS/SMA (PS6).

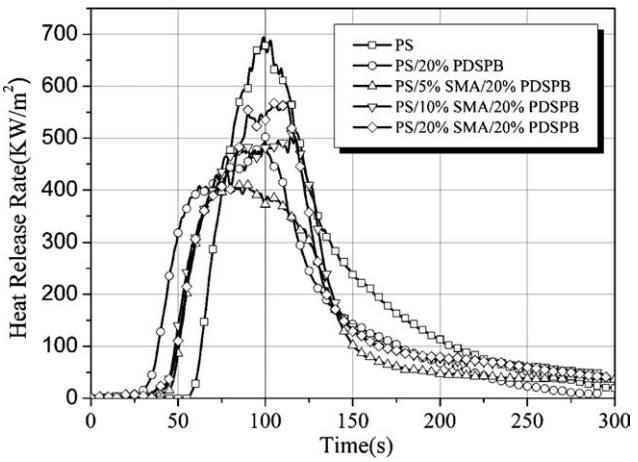

Figure 4 Heat release rate of pure PS, PS/20%PDSPB, PS/20%PDSPB/5%SMA, PS/20%PDSPB/10%SMA, and PS/20%PDSPB/20%SMA.

cone measurements. Heat release rate (HRR), in particular peak heat release rate (PHRR), has been found to be the most important parameter to evaluate fire safety.

Comparison of the HRR data for pure PS, PS/PDSPB, and PS/PDSPB/SMA blends is shown in Figure 4. Table III shows PHRR values of the samples.

Figure 4 shows that pure PS resin burns very fast after ignition and a sharp PHRR appears at 700 kW/m^2. When 20 wt % PDSPB is added (PS2), the value of PHRR decreases to 502 kW/m^2, which is 28% lower than pure PS. In PS/PDSPB/SMA systems, the PHRR of PS3 (5 wt % SMA) is reduced by 18% relative to PS/PDSPB blend. However, when the content of SMA is increased to 20 wt %, the PHRR is improved by 14% compared with PS/PDSPB blend. This indicates that 20 wt % contents of SMA are obviously excessive for reducing flame retardance. From the above it appears that in PS/PDSPB/SMA systems, 5 wt % content of SMA is adequate to reduce the PHRR. However, the ignition time of the PS/PDSPB samples (see Table III) is lower than that of pure PS. The reason may be due to the fact that PDSPB decomposes earlier than PS itself, and some small volatile molecules are produced from the decomposition of PDSPB. Similar phenomenon was observed by Ma et al.[7] and Song et al.[21] Whereas after compatibilization, the ignition time was higher than that for PS/PDSPB system and much higher with the decrease of SMA incorporation. The result indicates that compatibilization could delay thermal oxidation degradation of flame retardant PS, which has been reported in PP system by Song et al.[24]

Results with similar trend could be obtained from the LOI test, as shown in Table III. The LOI value of PS resin is 17.6, indicating its inherent flammability properties. When 20 wt % PDSPB is added, the flame retardancy of the PS blend is improved. At the same time, the dripping tendency during combustion becomes weaker. When 5 wt % SMA was loaded, the LOI kept in a relatively high value. However, as SMA increases, the LOI value of the blends decreases.

There is an optimum loading content of the compatibilizer for the flammability properties. This is because two effects were produced after the compatibilization. On the one hand, compatibilization can make the flame retardant PDSPB disperse uniformly. The more the compatibilizer added, the more evenly the flame retardants distributed. Therefore, the increase of the compatibilizer content is positive for improving the flame retardant properties. On the other hand, a ring opening reaction takes place between the $-NH_2$ functional groups of the flame retardant PDSPB, which play a role of gas source in IFR, and the MAH of the compatibilizer SMA after compatibilization, causing the absence of gas source. The more the compatibilizer added, the more the gas source lost. From this sense, the increase of the compatibilizer addition is negative for improving the flame retardant properties. Consequently, for the PS/PDSPB/SMA systems, a best flame retardant property is obtained at the SMA loading content of 5 wt %, when the two opposite effects are balanced.

TGA shown in Figure 5 can approximately describe the possible chemical reaction between the components with different SMA content when burning. The results show that two steps of degradation, one around 300–450°C and the other higher than 500°C, exist in the compatibilized system. The first step can be considered as the thermal degradation of PS resin, the same as pure PS1 and PS2 samples, which has been discussed previously.[10] In this step, the temperature at maximum degradation rate is increased and maximum degradation rate is reduced with the addition of 20% PDSPB. The second step from 450 to 550°C might be attributed to the degradation of more stable amide groups and imide

TABLE III
Peak Heat Release Rate, Time to Ignition and LOI Values of the Samples

Sample	PS1	PS2	PS3	PS4	PS5	PS6
PHRR (kW/m^2)	700 ± 21	502 ± 18	410 ± 13	509 ± 14	573 ± 16	713 ± 17
Time to ignition (s)	49 ± 1	25 ± 1	42 ± 2	34 ± 1	30 ± 0	49 ± 1
LOI	17.6	23.8	24.2	22.7	22.3	18.3

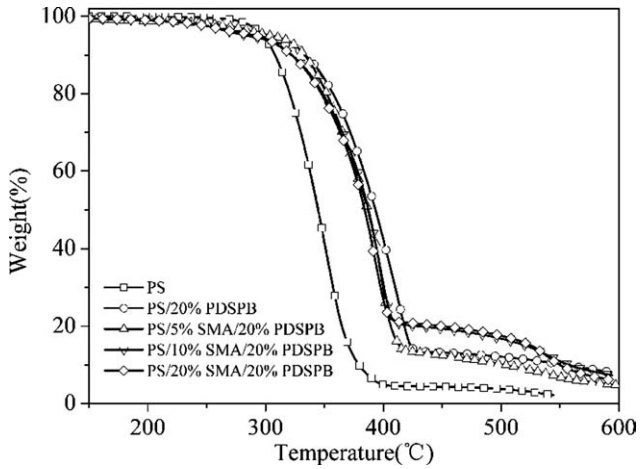

Figure 5 TGA curves of pure PS, PS/20%PDSPB, PS/20%PDSPB/5%SMA, PS/20%PDSPB/10%SMA, and PS/20%PDSPB/20%SMA.

groups as illustrated elsewhere.[25,26] This indicates that the —NH_2 groups dehydrating into more stable imide groups at high temperature is the reason for the gradual loss of gas source with the increase of SMA content.

The lack of gas source can be reflected visually from the microstructures of the residues. Figure 6 shows the morphologies of the chars after combustion for PS/PDSPB and PS/ PDSPB/SMA blends. The chars of PS2 and PS3 exhibit a honeycomb structure. Some cavities can be seen on the char surface. However, there is no honeycomb bubbles scatter on the char surface of PS4 and PS5. Our previous work has demonstrated that[7] an intumescent char with honeycomb structure could be formed during burning process, because the nonflammable gas released by gas source (—NH_2) can make the char swell. The formation of intumescent char is responsible for the flame retardancy. According to this, if some —NH_2 groups remain after melt blending (PS3), the intumescent char could form and the flammability could be reduced. Otherwise (PS4 and PS5), the flame retardancy will decrease. This is the reason why the flame retardant properties of PS3 are the best.

CONCLUSIONS

The relationship between the content of compatibilizer and the properties of the PS/PDSPB/SMA blends was investigated. SMA was used as the compatibilizer for flame retardant PS systems, in which MAH could react with functional groups (—NH_2) present on the flame retardant PDSPB to form *in situ* graft copolymer, whose chemical structure was verified. This compatibilization significantly reduced the size of the dispersed PDSPB domains and improved the interfacial adhesion between PS and PDSPB.

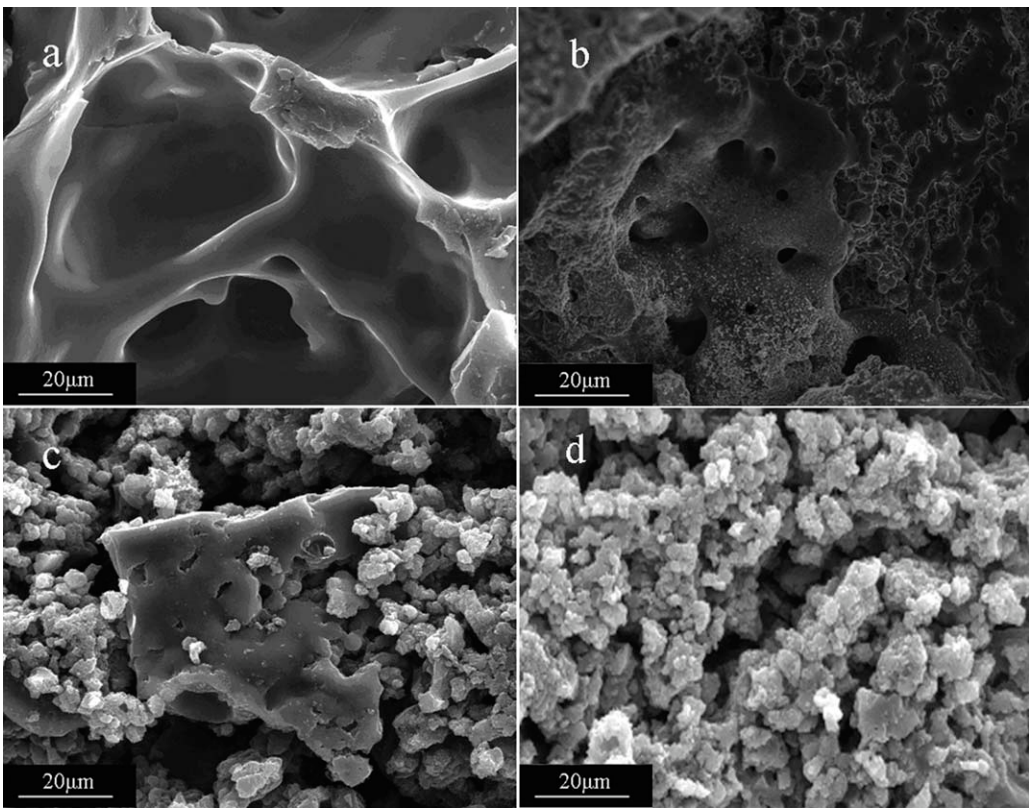

Figure 6 FESEM observations of residues from PS/20%PDSPB (a), PS/20%PDSPB/5%SMA (b), PS/20%PDSPB/10%SMA (c), and PS/20%PDSPB/20%SMA (d) after cone calorimetric measurements.

With the same PDSPB loading (20 wt %), addition of 5, 10, and 20 wt % SMA increased the impact strength of the flame retarded PS by about 29, 103, and 201%, respectively. The PHRR of PS/PDSPB/5 wt % SMA blends was reduced by 18.3% relative to PS/PDSPB blend. However, when the content of SMA was increased to 20 wt %, the PHRR was improved by 14.2% compared with PS/PDSPB blend. Results with similar trend were obtained from the LOI test. 5 wt % is the optimum SMA loading content to improve the mechanical properties and to reduce the flammability properties at the same time. Results of thermal gravimetric analysis revealed that the $-NH_2$ groups change into more stable imide groups at high temperature, causing the absence of gas source. Char morphologies collected after cone calorimetry show that the intumescent char couldn't form during combustion process because of the absence of gas source, which is the main reason for the deteriorate effect of high SMA loading.

References

1. Othman, N.; Ismail, H.; Mariatti, M. Polym Degrad Stab 2006, 91, 1761.
2. Modesti, M.; Lorenzetti, A.; Bon, D.; Besco, S. Polym Degrad Stab 2006, 91, 672.
3. Lai, S. M.; Li, H. C.; Liao, Y. C. Eur Polym J 2007, 43, 1660.
4. Shen, H.; Wang, Y. H.; Mai, K. C. Thermochim Acta 2009, 483, 36.
5. Bourbigot, S.; Le Bars, M.; Duquesne, S.; Rochery, M. Macromol Mater Eng 2004, 289, 499.
6. Tang, Y.; Hu, Y.; Wang, S. F.; Gui, Z.; Chen, Z. Y.; Fan, W. C. Polym Int 2003, 52, 1396.
7. Ma, H. Y.; Tong, L. F.; Xu, Z. B.; Fang, Z. P.; Jin, Y. M.; Lu, F. Z. Polym Degrad Stab 2007, 92, 720.
8. Ma, H. Y.; Tong, L. F.; Xu, Z. B.; Fang, Z. P. Appl Clay Sci 2008, 42, 238.
9. Ma, H. Y.; Tong, L. F.; Xu, Z. B.; Fang, Z. P. Adv Funct Mater 2008, 18, 414.
10. Chen, Y. J.; Fang, Z. P.; Yang, C. Z.; Wang, Y.; Guo, Z. H.; Zhang, Y. J Appl Polym Sci 2010, 115, 777.
11. Dedecker, K.; Groeninckx, G. Macromolecules 1999, 32, 2472.
12. Asthana, H.; Jayaraman, K. Macromolecules 1999, 32, 3412.
13. Cho, K.; Li, F. Macromolecules 1998, 31, 7495.
14. Cigana, P.; Favis, B. D.; Albert, C.; Vu-Khanh, T. Macromolecules 1997, 30, 4163.
15. Zhang, J. F.; Sun, X. Z. Macromol Biosci 2004, 4, 1053.
16. Dharmarajan, N.; Datta, S.; Ver Strate, G.; Ban, L. Polymer 1995, 36, 3849.
17. Beck Tan, N. C.; Tai, S. K.; Briber, M. Polymer 1996, 37, 3509.
18. Mulkern, T. J.; Beck Tan, N. C. Polymer 2000, 41, 3193.
19. Monticelli, O.; Fina, A.; Ullah, A.; Waghmare, P. Macromolecules 2009, 42, 6614.
20. Fina, A.; Tabuani, D.; Peijs, T.; Camino, G. Polymer 2009, 50, 218.
21. Song, P. A.; Shen, Y.; Du, B. X.; Peng, M.; Shen, L.; Fang, Z. P. ACS Appl Mater Interface 2009, 1, 452.
22. Chiang, W. Y.; Hu, C. H. Eur Polym J 1999, 35, 1295.
23. Chiang, W. Y.; Hu, C. H. J Appl Polym Sci 1999, 71, 865.
24. Song, P. A.; Fang, Z. P.; Tong, L. F.; Xu, Z. B. Polym Eng Sci 2009, 49, 1326.
25. Gaina, V.; Gaina, C.; Stoleriu, A.; Timpu, D.; Sava, M.; Rusu, M. Polym Plast Technol Eng 1999, 38, 927.
26. Deng, R. S.; Wei, Y. F.; Chen, B. N. Polyamide Resins and Their Applications; China Chemical Industry Press: Beijing, 2002; p 102.